Full-Sphere Sound Field of Constant-Beamwidth Transducer (CBT) Loudspeaker Line Arrays*

D. B. (DON) KEELE, JR., *AES Fellow*

Harman/Becker Automotive Systems, Martinsville, IN 46151, USA

The full-sphere sound radiation pattern of the constant-beamwidth transducer circular-wedge curved-line loudspeaker array exhibits a three-dimensional petal or eye-shaped sound radiation pattern that stays surprisingly uniform with frequency. Oriented vertically, it not only exhibits the expected uniform control of vertical coverage, but also provides significant coverage control horizontally. The horizontal control is provided by a vertical coverage that decreases smoothly as a function of the horizontal off-axis angle and reaches a minimum at right angles to the primary listening axis. This is in contrast to a straight-line array, which exhibits a three-dimensional sound field that is axially symmetric about its vertical axis and exhibits only minimal directivity in the horizontal plane due to the inherent directional characteristics of each of the sources that make up the array.

0 INTRODUCTION

Constant-beamwidth transducer (CBT) array theory is based on unclassified military underwater transducer research done in the late 1970s and early 1980s [1][2]. The research describes a curved-surface transducer in the form of a spherical cap with frequency-independent Legendre shading that provides wide-band extremely constant beamwidth and directivity behavior with virtually no sidelobes. In 2000 Keele applied the theory to loudspeaker arrays [3] where he extended the concept to arrays based on toroid-shaped curved surfaces and to circular-arc line arrays. He also extended the concept to straight-line and flat-panel CBT arrays with the use of signal delays [4]. The Appendix gives a brief review of CBT theory.

Traditionally line arrays are thought to provide directional control in one plane only. This is quite true for straight-line arrays, but not for curved-line ones. In addition to the expected coverage control in the plane of the curved array, the curvature of the line array also provides directional control at off-axis angles in the opposite planes. For the typical vertically oriented curved-line array this means that the array provides not only the expected directional control vertically, but also horizontally.

The horizontal directional control provided by the curvature of the line array is primarily exhibited by a narrowing vertical coverage as a function of the horizontal off-axis angle and an increasing level as the listener location proceeds off axis horizontally. In front of the curved-line array, along the primary listening axis, the curvature of the array places sources at different distances from the listening location and provides the primary directional control mechanism. However, for off-axis horizontal locations, the curvature of the array is less and less evident as one proceeds to greater off-axis horizontal angles. At $\pm 90°$ off axis horizontally, the curvature is entirely nullified and all sources are essentially equidistant from far-field listening or observation locations. At these locations the array appears essentially as a straight-line array, providing both maximum level and the narrowest possible vertical coverage. Interestingly the curved-line array thus provides its maximum intensity at right angles to its primary listening axis.

Further analysis of the CBT circular-wedge line array reveals that its vertical coverage gets narrower and narrower as one proceeds off axis horizontally. The narrowing of vertical coverage is found to follow the cosine of the off-axis horizontal angle. This means that the vertical coverage of the array narrows smoothly from its designed on-axis value and reaches a minimum at right angles horizontal to the primary listening axis.

The full-sphere sound field of the CBT curved-line array reveals a characteristic three-dimensional petal- or eye-shaped sound radiation pattern, which stays surprisingly uniform with frequency. This provides very uniform directivity and beamwidth control above a certain frequency set by the size of the array and its designed vertical coverage. Although the horizontal $\pm 90°$ off-axis intensity is higher than the primary designed listening axis, the effect is essentially negated because the vertical coverage

*Presented at the 114th Convention of the Audio Engineering Society, Amsterdam, The Netherlands, 2003 March 22–25.

of the array is the most narrow at these same extreme off-axis angles. This effect is also minimized by the reduced off-axis horizontal radiation of an array made of real-world loudspeakers.

This paper is organized as follows. Section 1 gives a description of the numerical simulator used to predict the radiation patterns of the arrays modeled, describes typical simulator outputs, and describes the three-dimensional axis and orientation for the polar balloon plots. Section 2 analyzes the predicted sound field of a conventional straight-line array designed to provide a controlled vertical coverage. Section 3 analyzes the sound field of two curved-line CBT arrays — the first designed to provide broad vertical coverage, and the second designed for narrow vertical coverage. The variation of the CBT curved-line array's vertical beamwidth as a function of the array's horizontal (azimuth) angle is analyzed in section 4. Section 5 concludes and Section 6 lists the references. The Appendix presents a review of CBT theory and a full set of polar balloons at octave center frequencies for both analyzed CBT arrays of Section 3.

1 ARRAY SIMULATOR

1.1 Description

The point-source array simulator program introduced in [3], [4] was used to predict the directional characteristics of the various arrays in this paper. This program calculates the pressure distribution at a specific distance (all simulations here are done at a far-field distance of 250 m) for a three-dimensional array of point sources of arbitrary magnitude and phase.

Polar rotations were all done around the center of the coordinate system. Note that all the conventional curved CBT arrays were offset so that their centers of curvature coincided with the center of the coordinate system.

Program outputs included the following:

1) Source configuration views as seen from front, top, and sides

2) Plots of horizontal and vertical beamwidths (-6 dB) versus frequency at each one-third-octave center from 20 Hz to 16 kHz

3) Plots of directivity index and Q versus frequency at each one-third-octave center from 20 Hz to 16 kHz

4) Plots of on-axis frequency response (loss) versus frequency, compared to all sources on and in phase at the pressure sampling point. (This plot indicates how much on-axis attenuation the array imposes as compared to the situation where all the sources add in phase at the sampling point.)

5) Complete set of three-dimensional polar balloons showing oblique, front, side, and top views at octave center frequencies (These polar balloons show the predicted three-dimensional sound field of any array with a shape based on a deformed sphere whose radius in a particular direction is proportional to the array's radiated level — in dB—in that particular direction. The shape is scaled linearly such that a radius of 1 corresponds to 0 dB, a radius of 0.5 dB corresponds to -20 dB, and a radius of 0 — (the center) — corresponds to a level of -40 dB).

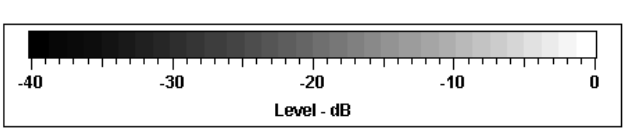

Fig. 1. Grayscale used for polar balloon plots. Scale varies smoothly from white at 0 dB through midlevel gray at -20 dB, to low-level black at -40 dB.

1.2 Shading

The dB levels of all the polar balloons in this paper are shaded according to the scale shown in Fig. 1.

1.3 Axis Orientation

The three-dimensional orthogonal axis system used in this study is shown in Fig. 2. All the arrays are constructed either on the Z axis (straight-line arrays) or on the $X-Z$ plane (curved-line arrays) with their axes facing in the positive X direction.

2 STRAIGHT-LINE ARRAY

To illustrate the directional pattern of a source that exhibits omnidirectional radiation in one plane and directional radiation in the other, a straight-line array was analyzed. The array is composed of 50 point sources distributed equally along a 0.3-m (13.5-in) distance on the Z axis centered on the $X-Y$ plane. The array is 1 wavelength high at 1 kHz.

The strengths of the sources have been adjusted to follow a Hann (cosine squared) window with the center source on full and the strengths of the remaining sources smoothly tapering to zero at the outside ends of the array. This shading minimizes sidelobes.

The close 6.8-mm (0.27-in) spacing of the sources ensures operation to above 20 kHz without grating lobes.

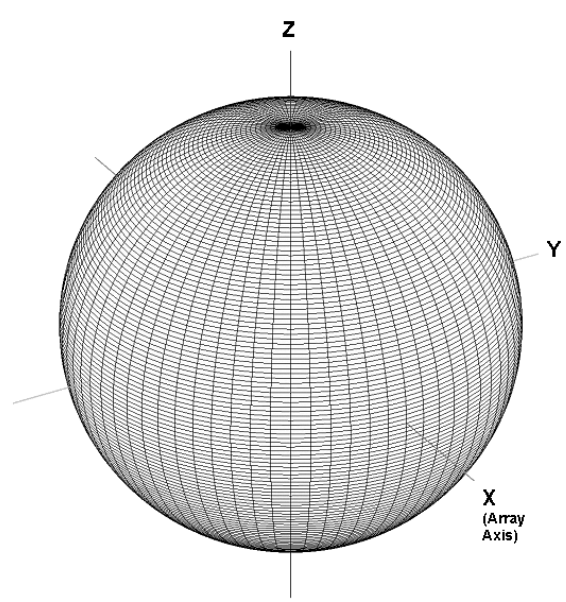

Fig. 2. Axis orientation for oblique views of polar balloon plots. Orientations are illustrated by directional pattern of an omnidirectional source (perfect spherical polar balloon). Orthogonal rectangular X–Y–Z axes are indicated. Array axis points in direction of the positive X axis.

Essentially this means that the line operates as a continuous source for frequencies below 20 kHz. Figs. 3–5 show side, front, and top views of the array.

The predicted vertical and horizontal beamwidth (−6 dB) of the array is shown in Fig. 6. Note that the horizontal beamwidth (circles) is constant at 360°, which indicates that the line's radiation is independent of direction in the horizontal plane (polar symmetry about the *Z* axis). The vertical beamwidth (triangles) indicate that the line's radiation narrows continually above 1 kHz, halving for each doubling of frequency.

The array's predicted directivity is shown in Fig. 7. It indicates a directivity index that rises at 10 dB per decade above 1 kHz.

The on-axis of the array (essentially the on-axis frequency response) is shown in Fig. 8. The curve is normalized to the level that results when all sources are on (at their shaded level) and in phase at the observation point. The straight-line array has no on-axis loss because all points of the array are essentially equidistant from a far-field point on its axis.

2.1 Broad Vertical Coverage Balloon Plots of Straight-Line Array

Polar balloons will illustrate the three-dimensional direction radiation of the line array of Fig. 3 at a frequency of 1.4 kHz, where the array exhibits a broad vertical beamwidth of 90°. These balloons are generated by calculating the response every 10° in azimuth (longitude) and every 2.5° in elevation (latitude). Figs. 9–11 show oblique, front (also side), and top views of the balloon. Refer to Section 1 for a description of the balloons and the shading.

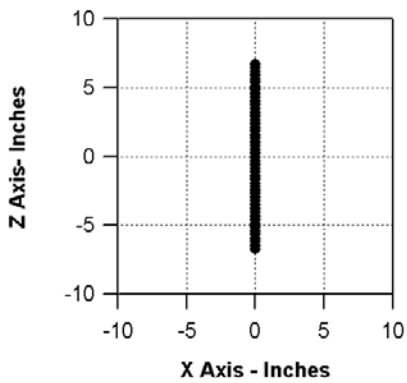

Fig. 3. Side view of straight-line array composed of 50 point sources. Array is 0.34-m (13.5-in) high (1 wavelength at 1 kHz) and is shaded with a Hann window (shading not indicated).

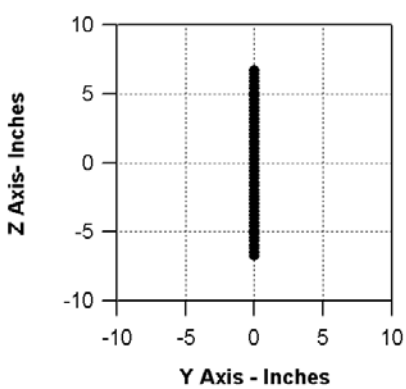

Fig. 4. Front view of array of Fig. 3.

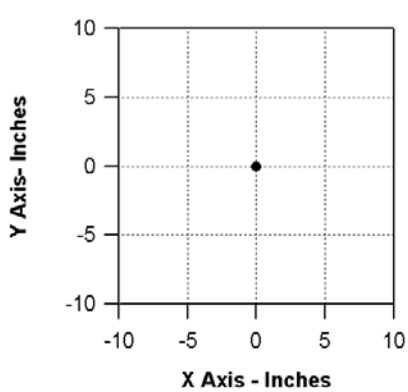

Fig. 5. Top view of array of Fig. 3.

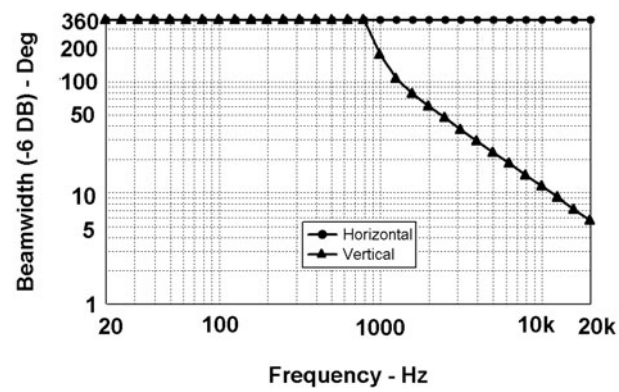

Fig. 6. Horizontal and vertical beamwidths (−6 dB) of array of Fig. 3. Note vertical narrowing above 1 kHz.

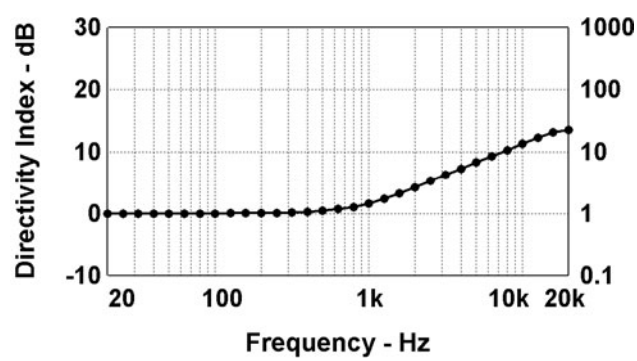

Fig. 7. Directivity index (left) and *Q* (right) of array of Fig. 3. Note increasing directivity above 1 kHz.

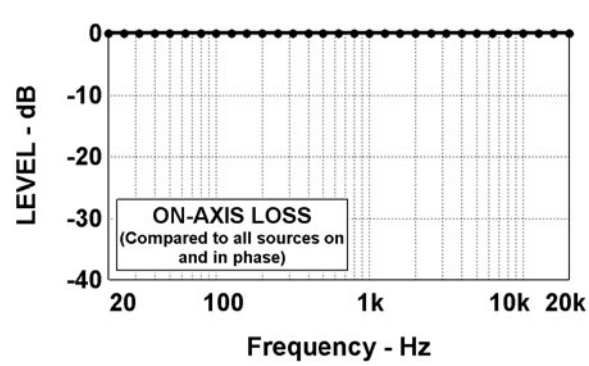

Fig. 8. On-axis loss of array of Fig. 3. This array exhibits no on-axis loss because all sources are essentially equidistant from the far-field observation location.

Note that the different views of the balloon illustrate the omnidirectional radiation of the array horizontally and the directional radiation vertically.

2.2 Narrow Vertical Coverage Balloon Plots of Straight-Line Array

Polar balloons will illustrate the three-dimensional directional radiation of the line array of Fig. 3 at a frequency of 5.3 kHz, where the array exhibits a narrow vertical beamwidth of 22.5°. These balloons are generated by calculating the response every 10° in azimuth (longitude) and every 2.5° in elevation (latitude). Figs. 12–14 show oblique, front (also side), and top views of the balloon. Refer to Fig. 1 for shading of the balloons.

These balloon views also illustrate the omnidirectional radiation of the array horizontally and the directional radiation vertically.

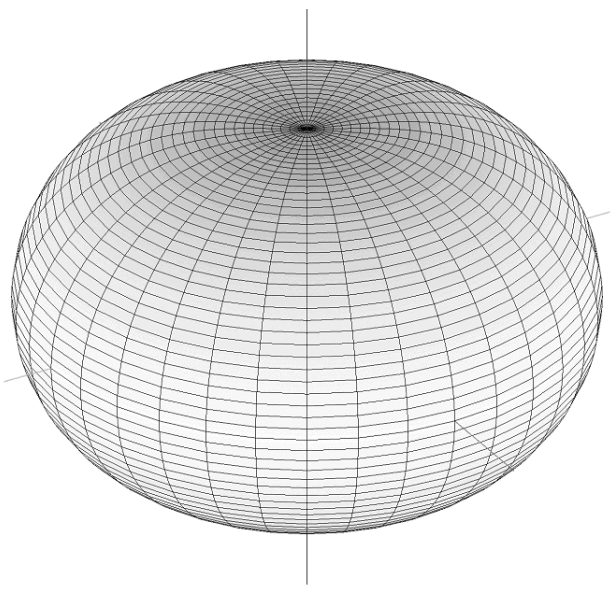

Fig. 9. Oblique view of polar balloon of straight-line array of Fig. 3 at 1.4 kHz where vertical coverage is 90°. Refer to Fig. 2 for axis orientation.

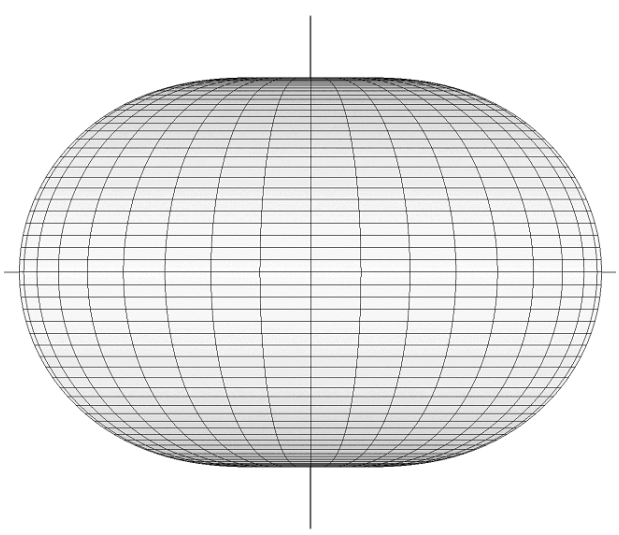

Fig. 10. Front (also side) view of polar balloon of straight-line array of Fig. 3 at 1.4 kHz. *X* (also *Y*) axis points out of the page. Note pumpkin shape, which indicates narrowing of vertical coverage.

3 CURVED-LINE CBT ARRAYS

The directional patterns of curved-line CBT arrays exhibit varying vertical coverage but not omnidirectional horizontal coverage. This is distinctly different than the

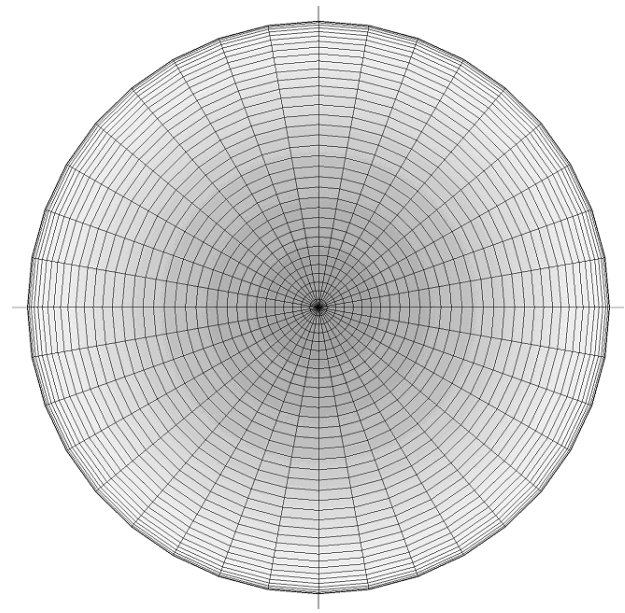

Fig. 11. Top view of polar balloon of straight-line array of Fig. 3 at 1.4 kHz. Note omnidirectional (circular) horizontal radiation. *Z* axis points out of the page.

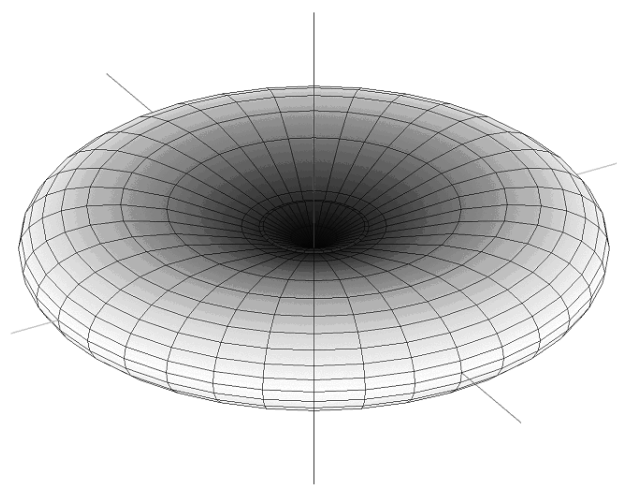

Fig. 12. Oblique view of polar balloon of straight-line array of Fig. 3 at 5.4 kHz, where vertical coverage is 22.5°. Refer to Fig. 2 for axis orientation. Donut shape indicates omnidirectional horizontal radiation and narrow vertical radiation.

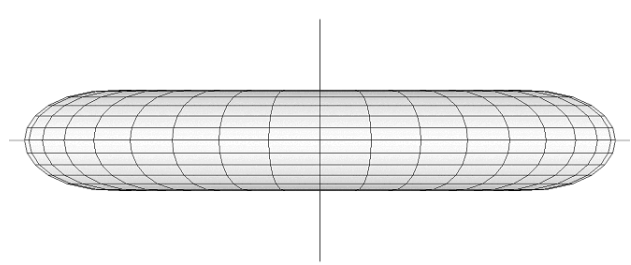

Fig. 13. Front (also side) view of polar balloon of straight-line array of FIg. 3 at 5.3 kHz. *X* (also *Y*) axis points out of the page.

behavior of the straight-line arrays. This behavior is investigated by analyzing the full-sphere radiation characteristics of two curved-line CBT arrays — one designed for a broad 90° vertical coverage and the other for a narrow 22.5° vertical coverage. These arrays are described in the following two sections.

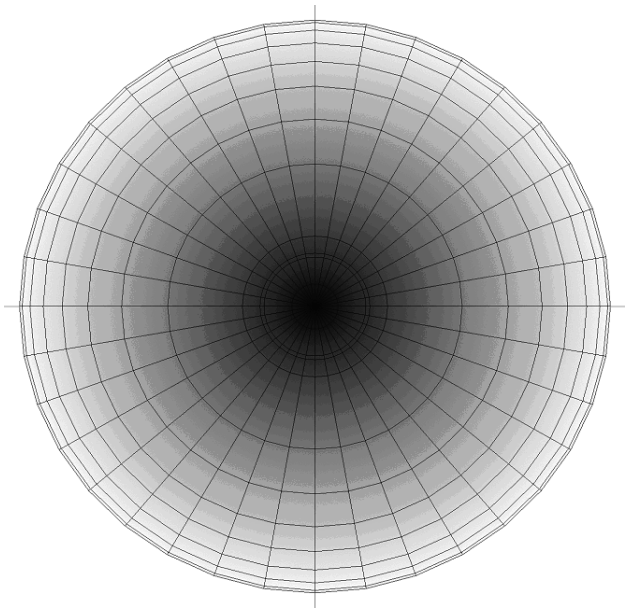

Fig. 14. Top view of polar balloon of straight-line array of Fig. 3 at 5.3 kHz. Note omnidirectional (circular) horizontal radiation.

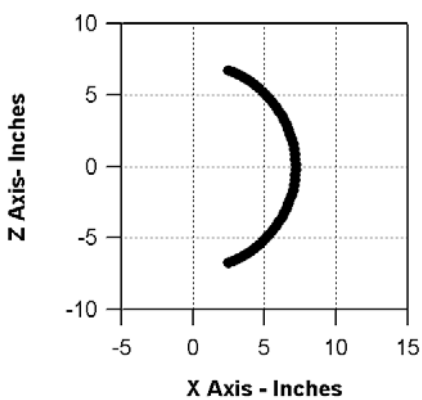

Fig. 15. Side view of 140° curved-line CBT array providing a broad vertical coverage of 90° made up of 50 point sources. Array is 0.34-m (13.5-in) high (1 wavelength at 1 kHz). Array center of curvature is located at origin. Array points toward right in the direction of the positive X axis.

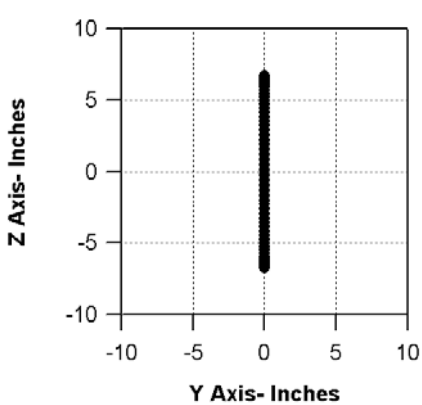

Fig. 16. Front view of CBT array of Fig. 15.

3.1 Broad Vertical Coverage CBT Array

This array is designed to provide a broad 90° vertical coverage on axis at frequencies above 1 kHz. As will be shown, the vertical coverage angle of the CBT curved-line array is not constant but changes as a function of the horizontal off-axis angle.

The array is composed of 50 point sources distributed equally around a 140° circular arc of 0.34-m (13.5-in) height located on the $Z-X$ plane. The center of curvature of the arc is located at the origin. The arc radius is 182-mm (7.18-in).

With Legendre shading [Eqs. (1) and (3) in the Appendix] of the strengths of the point sources, this array will then exhibit an on-axis vertical beamwidth of about 90° which is roughly 64% of the arc angle ($= 0.64 \times 40°$). As before, the array is one wavelength high at 1 kHz. Also, the close spacing of the sources ensures that the line essentially behaves continuously up to 20 kHz.

Figs. 15–17 show side, front, and top views of the array.

Fig. 18 shows the predicted vertical and horizontal beamwidths (−6 dB) of the CBT array of Fig. 15. Note the extremely uniform vertical beamwidth of the array above 1 kHz. Although the horizontal beamwidth is constant at 360°, this does not imply that the horizontal coverage is independent of direction in the horizontal plane. This is in stark contrast to the behavior of the straight-line array of Fig. 3. As will be shown shortly, the vertical beamwidth of the curved-line CBT array is a function of the horizontal (azimuth) angle.

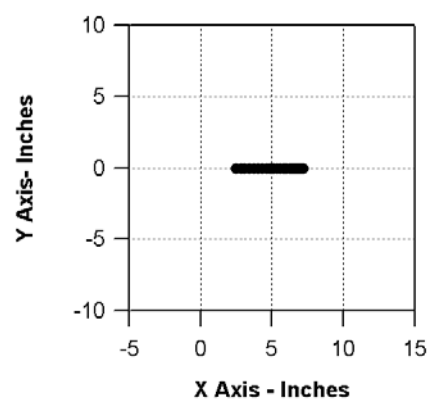

Fig. 17. Top view of CBT array of Fig. 15.

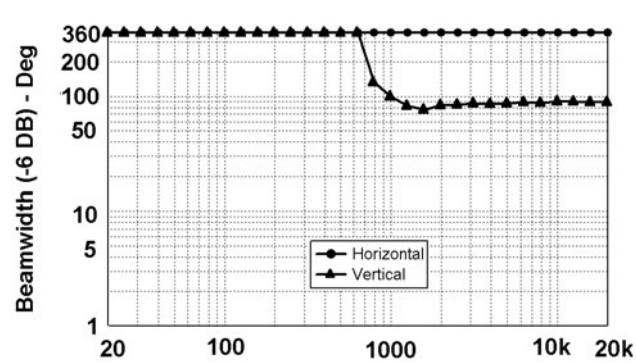

Fig. 18. Horizontal and vertical beamwidths (−6 dB) of CBT array of Fig. 15.

Fig. 19 indicates the CBT array's predicted directivity. The directivity is quite uniform above 1 kHz, although it exhibits a low directivity index which remains within 2.1–2.9 dB between 1 and 20 kHz.

Fig. 20 shows the on-axis loss of the broad-coverage CBT array. The curved-line CBT array exhibits loss above 1 kHz due to the curvature of the array. Above 1 kHz the on-axis response rolls off at 10 dB per decade because the sources are at different distances from the observation point.

3.2 Broad Vertical Coverage CBT Balloon Plots

Polar balloons will illustrate the three-dimensional directional radiation of the curved-line CBT array of Fig. 15 at a frequency of 8 kHz. This high frequency was chosen to display properly all the features of the array's radiation. Refer to the Appendix for a complete set of balloons at octave centers from 500 Hz to 16 kHz.

The balloons are generated by calculating the response every 5° in azimuth (longitude) and every 1.25° in elevation (latitude). Figs. 21–24 show oblique, front, side, and top views of the balloon. Refer to Fig. 1 for shading of the balloons.

The oblique view shown in Fig. 21 illustrates all the unusual features of the radiation pattern of the curved-line CBT array. The axis of the array points down and to the right (see Fig. 2 for orientation). Note several features of the display:

1) The smooth rounded surface of constant level in the forward (and rearward because the radiation is bidirectional) facing directions, which implies even coverage

2) The reduction of vertical beamwidth as one gets farther off axis horizontally

3) The very narrow vertical coverage at ±90° off axis horizontally

4) The sharp reduction of level in the *Y–Z* plane (up–down and right–left) except for narrow high-level projections in the extreme lateral directions at ±90° off axis horizontally.

The front view shown in Fig. 22 illustrates the peculiar petal or eyeball shape of the radiation. Note that the highest levels of the radiation are at right angles (±90° horizontal) to the on-axis direction (which faces straight out of the page). Note also that these high-level directions are accompanied by very narrow vertical coverage (only about 5° at this frequency). As noted before, the reduced off-axis horizontal radiation of real-world loudspeakers will also minimize this effect.

The side view shown in Fig. 23 illustrates the sharp reduction in level in the *Y–Z* plane (up–down and in and out of the page) and the dumb bell or petal shape of the pattern. Note also the high intensity level and narrow vertical beamwidth at right angles to on axis (in and out of the page).

The top view of Fig. 24, again shows clearly the high-intensity nubs (right–left) at right angles to on axis (up–down). As with all CBT arrays composed of point sources, the top view illustrates the forward–reverse symmetry of the CBT radiation.

3.3 Narrow Vertical Coverage CBT Array

This array is designed to provide a narrow vertical coverage of 22.5° on axis at frequencies above 1 kHz. The

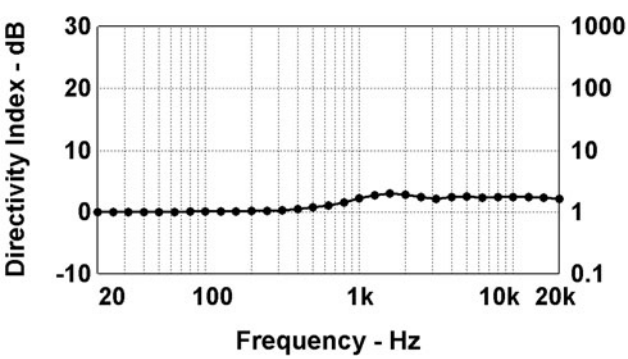

Fig. 19. Directivity index (left) and *Q* (right) of CBT array of Fig. 15.

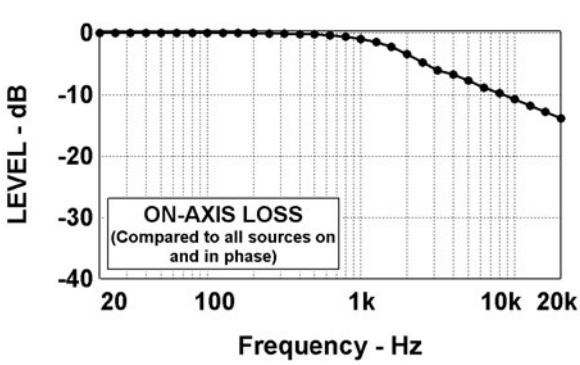

Fig. 20. On-axis loss of CBT array of Fig. 15. CBT array exhibits loss above 1 kHz due to array curvature.

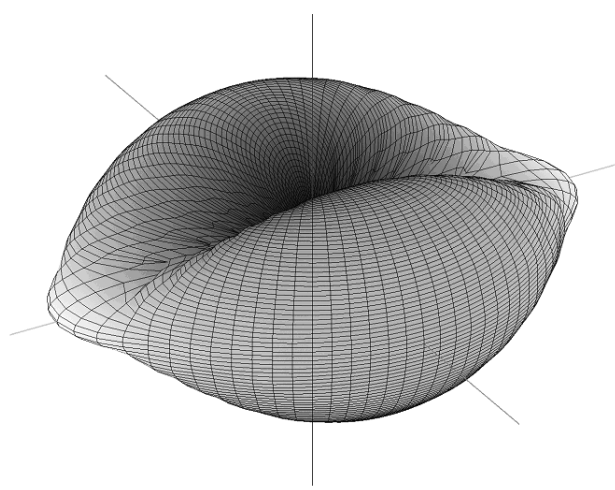

Fig. 21. Oblique view of polar balloon of 140° CBT line array of Fig. 15 at 8 kHz. Refer to Fig. 2 for axis orientation.

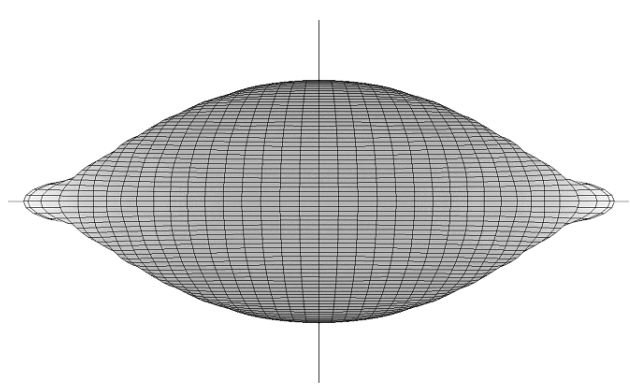

Fig. 22. Front view of polar ballon of 140° CBT line array of Fig. 15 at 8 kHz. *X* axis point out of the page.

array is composed of 200 point sources distributed equally around a 35° circular arc of 1.37-m (54-in) height located on the $Z-X$ plane. The center of curvature of the arc is located at the origin. The arc radius is 2.28-m (89.79-in).

Because of the narrow vertical coverage of this array (which is one-fourth that of the previous array), the height of the array is made four times that of the previous array in order to control the vertical beamwidth down to the same frequency. This array is one wavelength high at 250 Hz or four wavelengths at 1 kHz. The close spacing of sources ensures that the line essentially behaves continuously up to 20 kHz.

Figs. 25–27 show side, front, and top views of the array.

Fig. 28 shows the predicted vertical and horizontal beamwidths (−6 dB) of the narrow vertical coverage array. Note the extremely uniform vertical beamwidth of the array above 1 kHz. As before, although the horizontal beamwidth is constant at 360°, this does not imply that the horizontal coverage is independent of direction in the horizontal plane.

Fig. 29 indicates the CBT array's predicted directivity as a function of frequency. The directivity is quite uniform

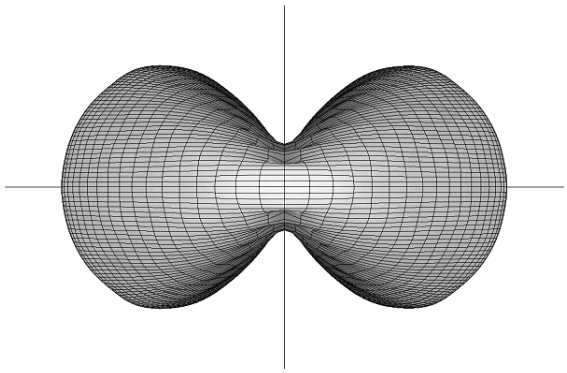

Fig. 23. Side view of polar balloon of 140° CBT line array of Fig. 15 at 8 kHz. X axis points toward right.

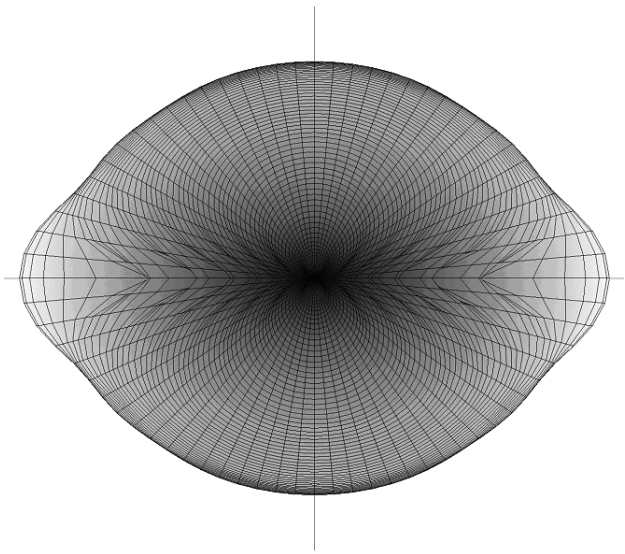

Fig. 24. Top view of polar balloon of 140° CBT line array of Fig. 15 at 8 kHz. X axis points down and Z axis points out of the page. Note that highest levels of radiation pattern are at right angles (±90° horizontal, right–left in display) to defined on-axis direction (up or down in display).

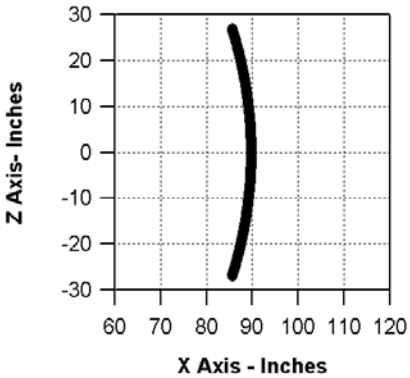

Fig. 25. Side view of 35° CBT line array providing a narrow vertical coverage of 22.5° made up of 200 point sources. Array is 1.37-m (54-in) height (4 wavelengths at 1 kHz). Array center of curvature is located at origin. Array points toward right in direction of the positive X axis.

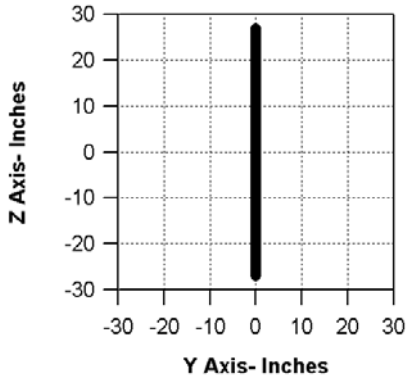

Fig. 26. Front view of CBT array of Fig. 25.

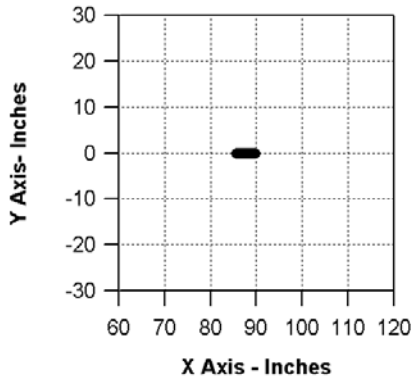

Fig. 27. Top view of CBT array of Fig. 25.

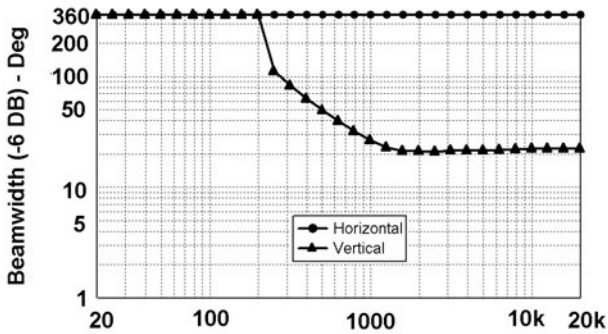

Fig. 28. Horizontal and vertical beamwidths (−6 dB) of CBT array of Fig. 25.

above 1 kHz, fitting within a 7.2 – 8.7 -dB window between 1 and 20 kHz.

Fig. 30 shows the on-axis loss of the narrow-coverage CBT array. The curved-line CBT array exhibits loss above 1 kHz due to the curvature of the array. Above 1 kHz the on-axis response rolls off at 10 dB per decade. Note that this figure is identical to the on-axis loss of the previous array (Fig. 20) because the operating bandwidths of the two are identical.

3.4 Narrow Vertical Coverage CBT Balloon Plots

Polar balloons will illustrate the three-dimensional directional radiation of the curved-line CBT array of Fig. 25 at a frequency of 8 kHz. This high frequency was chosen to display properly all the features of the array's radiation. Refer to the Appendix for a complete set of balloons at octave centers from 500 Hz to 16 kHz.

The balloons are generated by calculating the response every 5° in azimuth (longitude) and every 1.25° in elevation (latitude). Figs. 31–34 show oblique, front, side, and top views of the balloon. Refer to Fig. 1 for shading of the balloons.

The oblique view shown in Fig. 31 illustrates all the unusual features of the radiation pattern of the curved-line CBT array. Refer to the previous comments about the unusual features of these radiation patterns listed for Fig. 21.

Fig. 32 illustrates the peculiar petal or eyeball shape of the forward radiation. Refer to text comments on Fig. 22. Note the extreme narrow coverage to the sides.

The side view shown in Fig. 33 illustrates much the same features as Fig. 23 and described previously.

The top view in Fig. 34 also illustrates much the same features as Fig. 24.

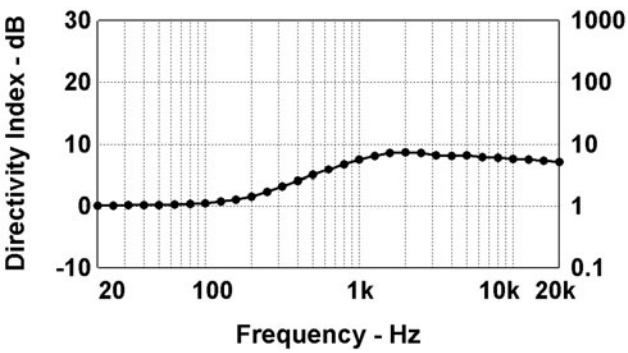

Fig. 29. Directivity index (left) and Q (right) of CBT array of Fig. 25.

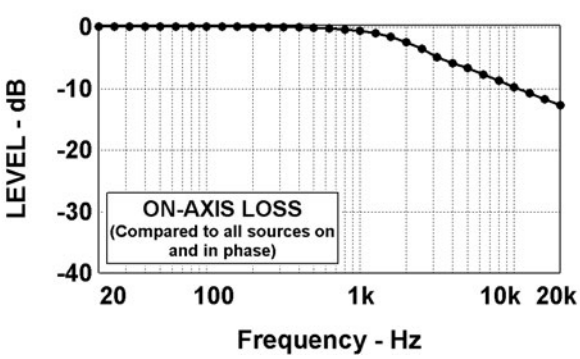

Fig. 30. On-axis loss of array of Fig. 25. Note that the loss of this array is identical to that of the previous array (Fig. 20) because both operate over the same frequency range.

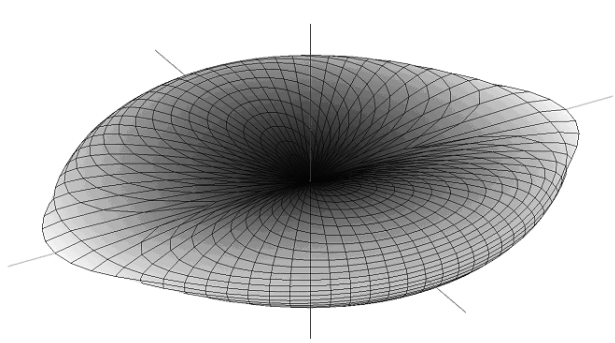

Fig. 31. Oblique view of polar balloon of 35° CBT line array of Fig. 25 at 8 kHz. Refer to Fig. 2 for axis orientation.

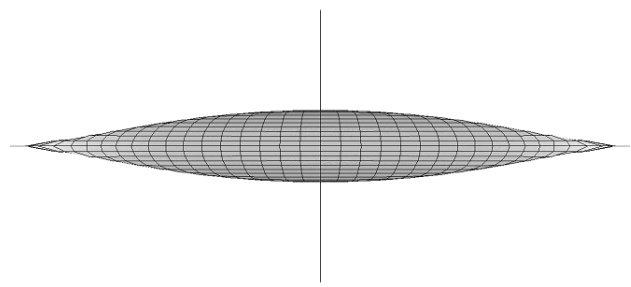

Fig. 32. Front view of polar balloon of 35° CBT line array of Fig. 25 at 8 kHz. X axis points out of the page.

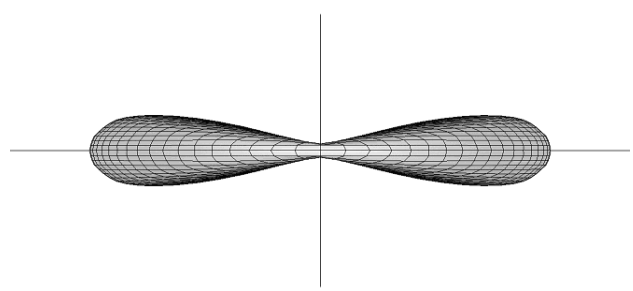

Fig. 33. Side view of polar balloon of 35° CBT line array of Fig. 25 at 8 kHz. X axis points toward right.

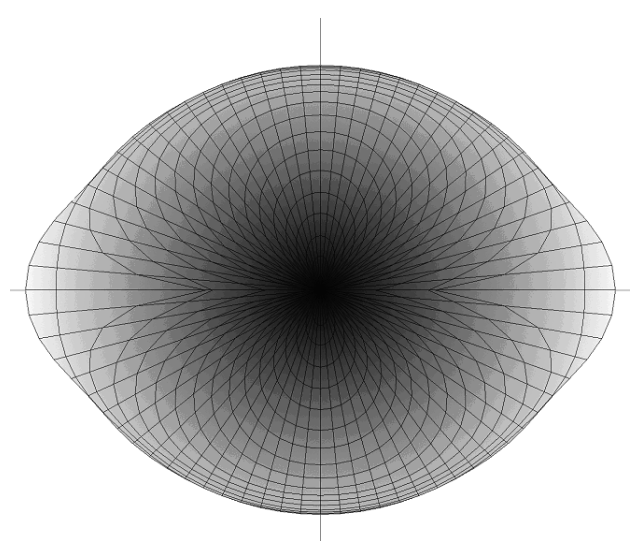

Fig. 34. Top view of polar balloon of 35° CBT line array of Fig. 25 at 8 kHz. X axis points down and Z axis points out of the page.

4 VARIATION OF CBT LINE ARRAY VERTICAL BEAMWIDTH WITH AZIMUTH ANGLE

This section analyzes the variation of the vertical beamwidth with the horizontal (azimuth) angle. The vertical beamwidth data were found to fit a cosine variation of the horizontal angle.

4.1 Simulating Vertical Beamwidth at Different Horizontal Off-Axis Angles

The broad vertical coverage CBT array of Fig. 15 was analyzed to generate several beamwidth versus frequency plots at several off-axis horizontal directions, including 0, ±15°, ±30°, ±45°, ±60°, ±75°, ±80°, ±85°, and ±90°. These plots, presented in Fig. 35, show that the vertical beamwidth diminishes progressively as you proceed off axis horizontally.

At ±90° off axis the curved-line array essentially appears as a straight-line array whose vertical beamwidth decreases continually with frequency. This deceasing bandwidth versus frequency characteristic acts as an asymptote for the vertical beamwidth plots at intermediate horizontal off-axis angles.

Fig. 36 shows the beamwidth values at the listed horizontal off-axis angles of Fig. 35 at the frequency of 16 kHz (dotted curve). The solid curve gives the best-fit cosine variation curve for an initial angle of 92.5°. This shows that the vertical beamwidth of the curved-line CBT array essentially follows a cosine variation decrease with off-axis horizontal angle.

4.2 Frontal Beam Shape

Assuming a cosine variation of the vertical beamwidth with horizontal off-axis angle, as determined in the previous section, a frontal beam shape can be derived, as shown in Fig. 37.

5 CONCLUSIONS

This paper has investigated the three-dimensional radiation pattern of curved-line CBT circular-arc array through simulations based on arrays of point sources. It was shown that the radiation pattern is completely unlike

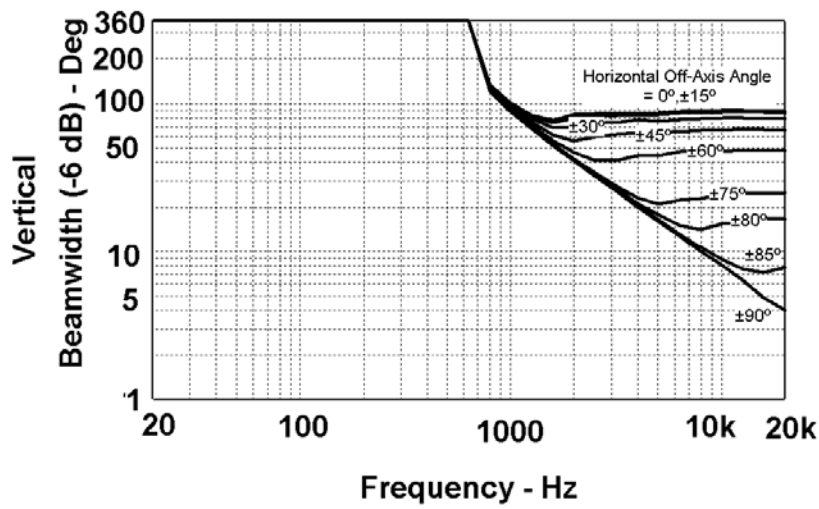

Fig. 35. Plot of vertical beamwidth (−6 dB) versus frequency at several different horizontal (azimuth) off-axis angles for broad-coverage CBT line array of Fig. 15. Note that vertical beamwidth narrows as you go off axis horizontally, but only to an asymptote that represents the beamwidth versus frequency of a straight-line array of the same height as the CBT array.

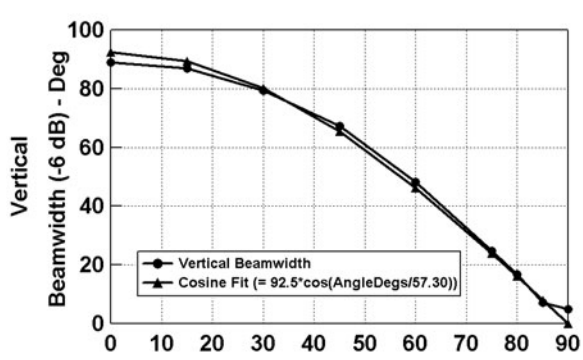

Fig. 36. Comparison of vertical beamwidth data of Fig. 35 at 16 kHz and a cosine variation best fit.

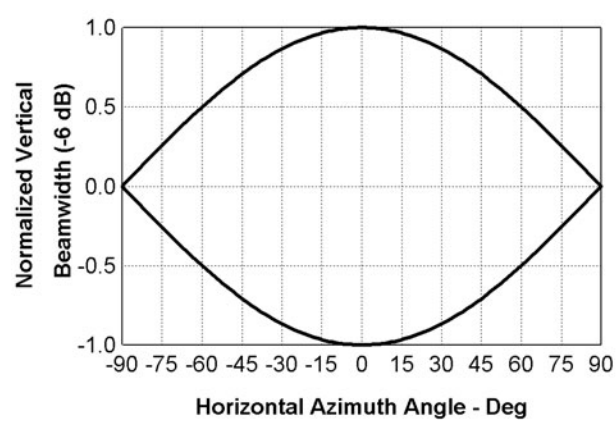

Fig. 37. Theoretical frontal beam shape of a curved-line CBT array looking somewhat petal- or eye-shaped. Plot reflects how CBT array vertical beamwidth changes as a function of horizontal azimuth angle, reaching a small value at right angles to on axis (±90° off axis horizontal), and follows a cosine relationship. Compare with Figs. 22 and 32.

the pattern of a conventional straight-line array that exhibits controlled vertical coverage but completely uncontrolled omnidirectional horizontal coverage with a pattern that is symmetric around the vertical axis.

Although still a line source, the curved-line CBT array shows significant horizontal directivity in addition to its expected vertical control. This horizontal directivity is exhibited by its variation of vertical beamwidth with the horizontal off-axis angle. The vertical beamwidth varies smoothly from the full value on axis to a low minimum value at right angles to the array's forward axis in a manner that follows the cosine of the off–axis horizontal angle.

Interestingly the curved-line array provides its maximum intensity at right angles (±90° off axis horizontally) to its primary defined axis. This is because all the sources that make up the array are essentially equidistant from the observation point and hence in phase at these angles. This feature does however, not upset the controlled and smooth frontal coverage and directivity of the array because these regions of highest level are confined to very small regions on the sides of the radiation pattern. Arrays made of real-world loudspeakers will also minimize this effect because of their reduced off-axis horizontal coverage.

The curved-line CBT array provides surprisingly constant directivity and uniform vertical beamwidth above a frequency related to the size of the array and its vertical coverage angle. This is accomplished without any complicated frequency-dependent signal processing. The only processing required is simple frequency-independent gain adjustment of levels of individual drivers to accomplish the Legendre shading.

6 REFERENCES

[1] P. H. Rogers and A. L. Van Buren, "New Approach to a Constant Beamwidth Transducer," *J. Acoust. Soc. Am.*, vol. 64, pp. 38–43 (1978 July).

[2] A. L. Van Buren, L. D. Luker, M. D. Jevnager, and A. C. Tims, "Experimental Constant Beamwidth Transducer," *J. Acoust. Soc. Am.*, vol 73, pp. 2200–2209 (1983 June).

[3] D. B. Keele, Jr., "The Application of Broadband Constant Beamwidth Transducer (CBT) Theory to Loudspeaker Arrays," presented at the 109th Convention of the Audio Engineering Society, *J. Audio Eng. Soc. (Abstracts)*, vol. 48, pp. 1104–1105 (2000 Nov.), Preprint 5216.

[4] D. B Keele, Jr., "Implementation of Straight-Line and Flat-Panel Constant Beamwidth Transducer (CBT) Loudspeaker Arrays Using Signal Delays," presented at the 113th Convention of the Audio Engineering Society, *J. Audio Eng. Soc. (Abstracts)*, vol. 50, pp. 958 (2002 Nov.), Convention Paper 5653.

APPENDIX

A.1 Review of CBT Theory

Quoting from Keele [3, section 1]:

> Rogers and Van Buren [1], and Van Buren et. al. [2] describe the theory and experiments of what they call broadband 'constant beamwidth transducers' (CBT) for use as underwater projectors and receivers for sonar use. Here the transducer is in the form of a circular spherical cap of arbitrary half angle whose normal surface velocity (or pressure) is shaded with a Legendre function. The Legendre shading is independent of frequency. This transducer provides a broadband symmetrical directional coverage whose beam pattern and directivity is essentially independent of frequency over all frequencies above a certain cutoff frequency, and also change very little with distance from the source. The transducer can be designed to cover any arbitrary coverage angle with a constant beamwidth that extends over an operating bandwidth which is, in theory, virtually unlimited.
>
> Rogers and Van Buren [1] determined that if the radial velocity (or equivalently the surface pressure) on the surface of a rigid sphere of radius *a* conforms to
>
> $$u(\theta) = \begin{cases} P_\nu(\cos\theta) & \text{for} \quad \theta \leqslant \theta_0 \\ 0 & \text{for} \quad \theta > \theta_0 \end{cases} \tag{1}$$
>
> where
>
> u = radial velocity distribution
> θ = elevation angle in spherical coordinates ($\theta = 0$ is center of circular spherical cap)
> θ_0 = half-angle of sperical cap
> P_ν = Legendre function of order ν ($\nu > 0$) of argument x
>
> then an approximation to the far-field pressure pattern, above a cutoff frequency which depends on the size of the sphere and the wavelength, will be
>
> $$p(\theta) = \begin{cases} P_\nu(\cos\theta) & \text{for} \quad \theta \leqslant \theta_0 \\ 0 & \text{for} \quad \theta > \theta_0 \end{cases} \tag{2}$$
>
> where $p(\theta)$ = radial pressure distribution.
>
> This surprising result shows that the far-field sound pressure distribution is essentially equal to the pressure distribution on the surface of the sphere. Rogers and Van Buren also point out that because the surface pressure and velocity are nearly zero over the inactive part of the outside surface of the sphere, the part of the rigid spherical shell outside the spherical cap region can be removed without significantly changing the acoustic radiation. This means that the ideal constant beamwidth behavior of the spherical cap is retained even though the rest of the sphere is missing!
>
> The Legendre function $P_\nu(\cos\theta)$ is equal to 1 at $\theta = 0$ and has its first zero at angle $\theta = \theta_0$, the half-angle of the spherical cap. The Legendre function order ν is chosen so that its first zero occurs at the half-angle of the spherical cap. Note that ν is normally greater than 1, and not necessarily an integer.
>
> Rogers and Van Buren also point out that the constant beamwidth behavior of a rigid spherical cap also applies as well to any acoustically transparent spherical shell. However the acoustic radiation is bidirectional, generating the same beam pattern front and rear.
>
> To sum up the advantages of CBT I quote from [1]:
>
> "We enumerate the expected properties of the CBT

above cutoff:

1) Essentially constant beam pattern.

2) Very low sidelobes.

3) The surface distribution as well as the pressure distribution at all distances out to the far-field is approximately equal to the surface distribution. Thus in a sense, there is no near-field.

4) Since both the surface velocity and surface pressure have the same dependence on θ, the local specific acoustic impedance is independent of θ (and equal to $\rho_0 c$). Thus the entire transducer is uniformly loaded."

Keele [3] extends the CBT theory to loudspeaker arrays and provides a simplified four-term series approximation to the Legendre shading of Eq. (1) which is acceptable over all useful Legendre orders:

$$U(x) \approx \begin{cases} 1 + 0.066x - 1.8x^2 + 0.743x^3 & \text{for} \quad x \leqslant 1 \\ 0 & \text{for} \quad x > 1 \end{cases} \tag{3}$$

where $x =$ normalized angle (θ/θ_0).

Note that this function is exactly 1 at $x = 0$ and 0 at $x = 1$ (where $\theta = \theta_0$ the half-angle of the cap). All the following simulations use Eq. (3) as a substitute for the Legendre function of Eq. (1). Between $x = 0$ and $x = 1$, Eq. (3) decreases monotonically and passes through 0.5 (-6 dB) at $x = 0.638$ which defines the CBT array's beamwidth (-6 dB) as being 64% of the array's arc angle.

As pointed out in [3], the coverage angle (6-dB down beamwidth) of the CBT array is approximately 64% of the cap angle or circular-arc angle.

Keele [3] also extends the CBT theory to circular arc line arrays. Here the array is a circular arc or wedge, usually oriented with its long axis vertical. The present paper analyzes the three-dimensional radiation pattern of this type of array.

A.2 Full Set Of Polar Balloons For CBT Arrays

Figs. 38 and 39 show the predicted three-dimensional polar responses of the CBT arrays of Figs. 15 and 25. The

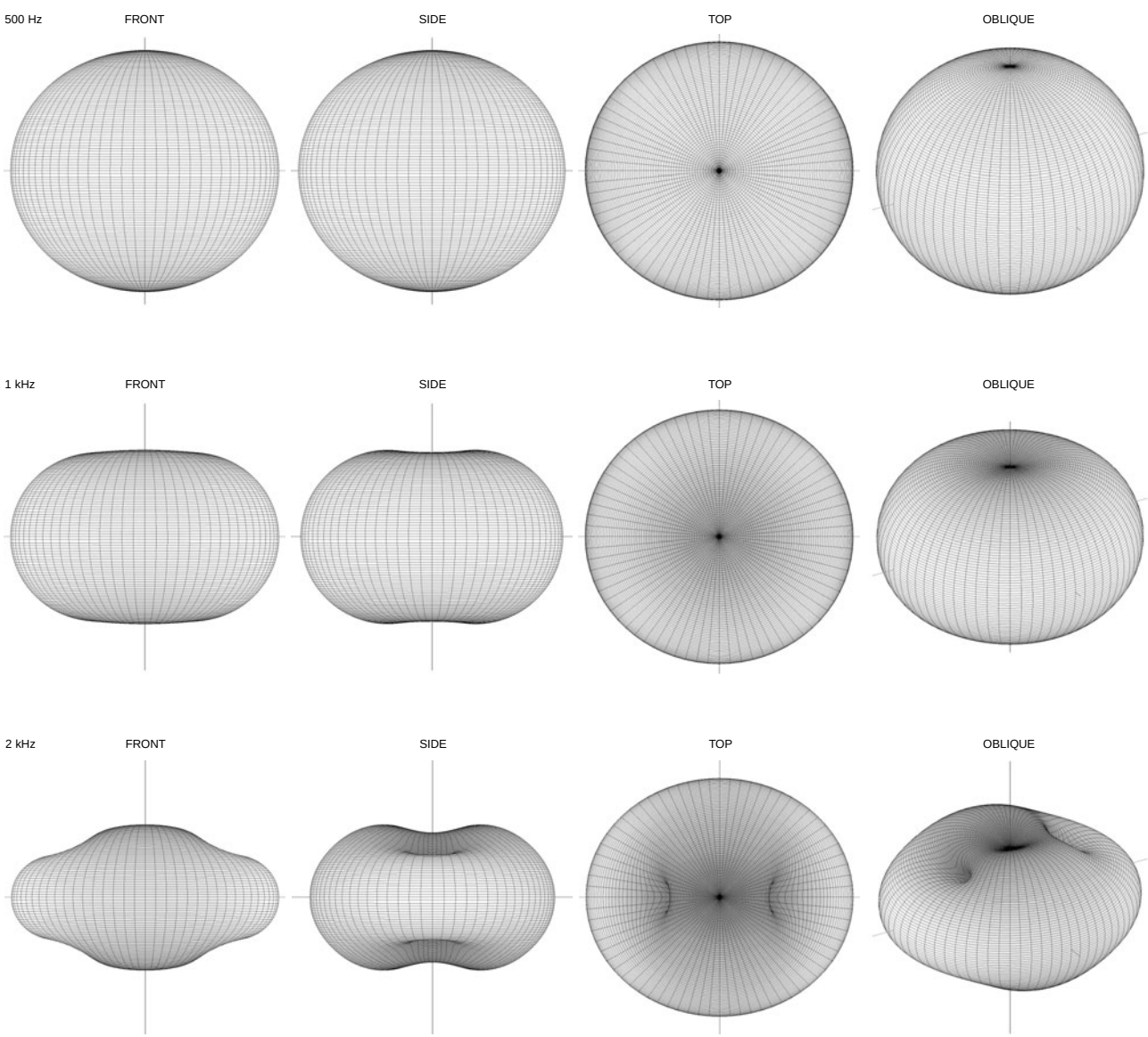

Fig. 38. Balloon plots for broad vertical coverage CBT line array of Fig. 15.

polar balloons are calculated at every octave center frequency from 500 Hz to 16 kHz. The balloons are derived by calculating the response every 5° in azimuth (longitude) and every 1.25° in elevation (latitude). The array axis points in the direction of the positive *X* axis (toward the equator). Front, side, top, and oblique views are shown. Refer to Fig. 1 for shading of these balloons and to Fig. 2 for the axis orientation.

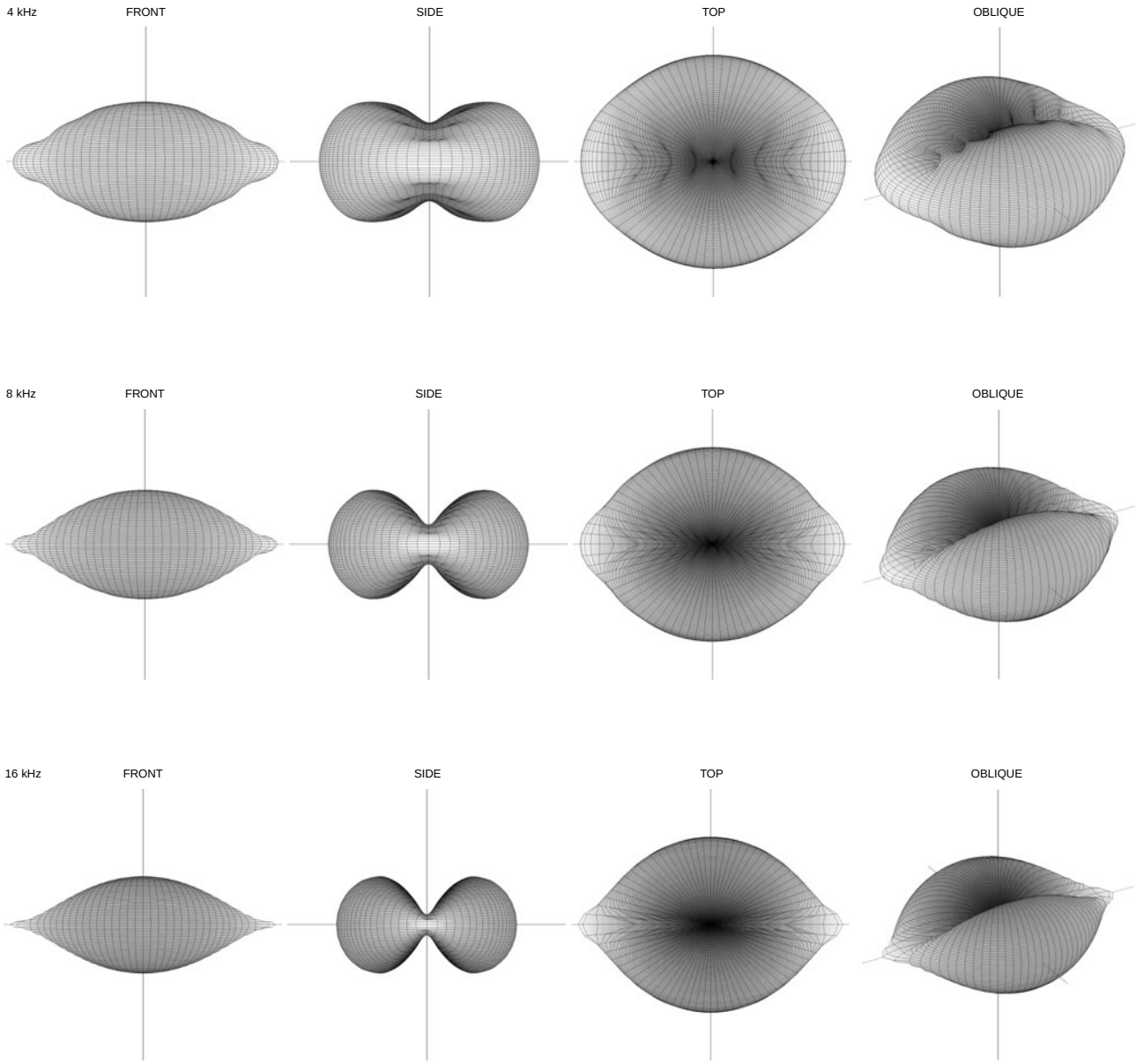

Fig. 38. *Continued*

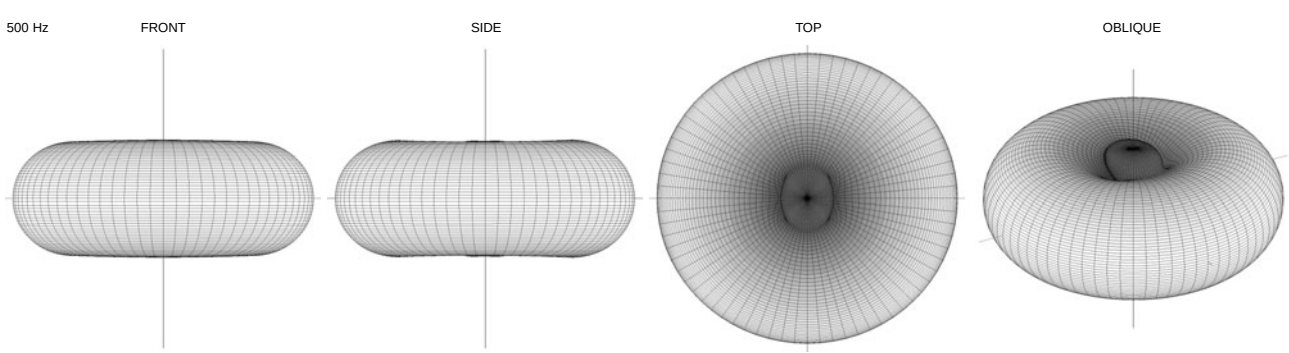

Fig. 39. Balloon plots for narrow vertical coverage CBT line array of Fig. 25.

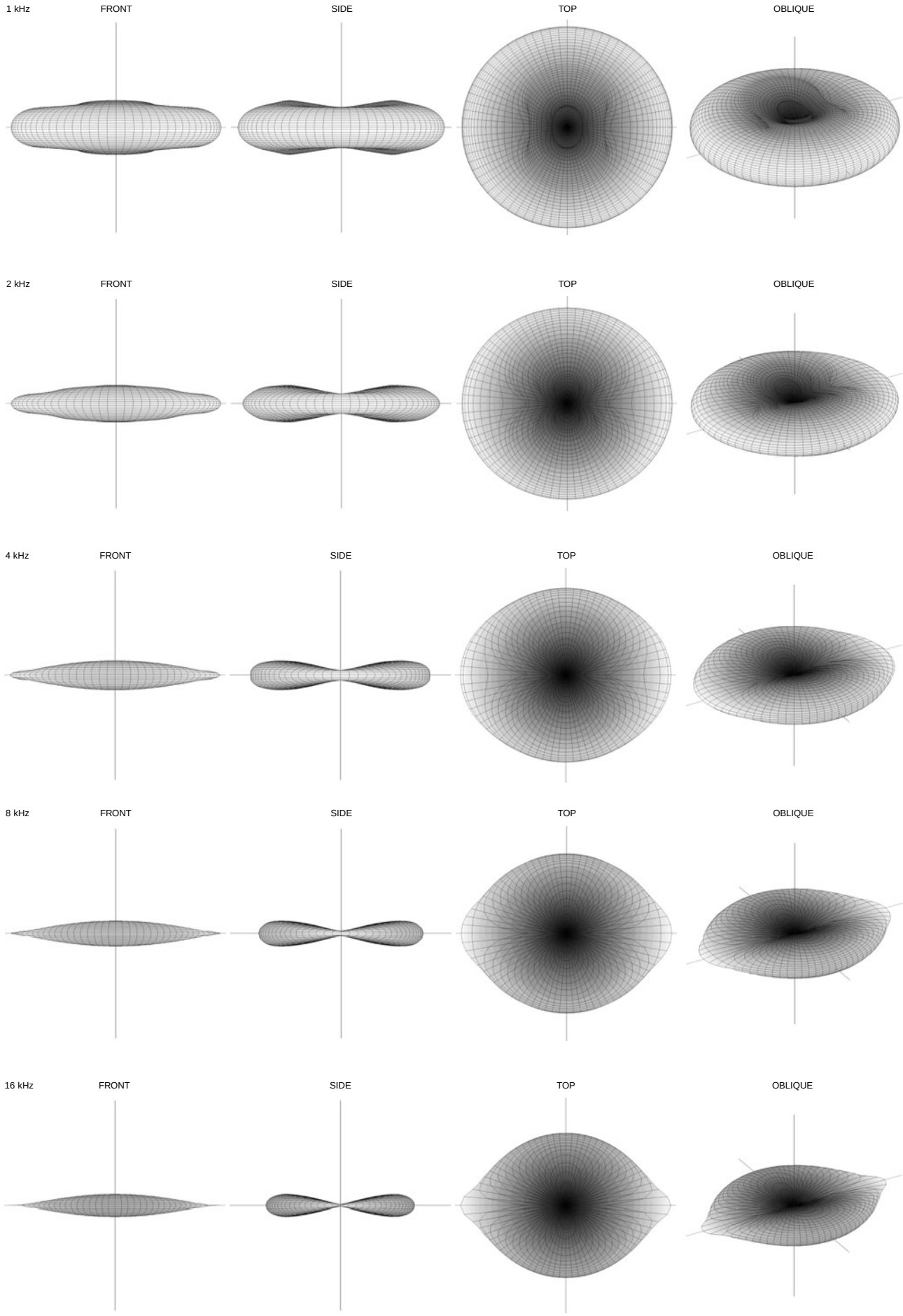

Fig. 39. *Continued*

THE AUTHOR

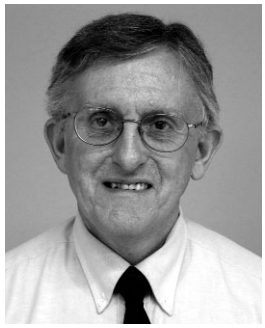

D. B. (Don) Keele, Jr. was born in Los Angeles, California, on 1940 November 2.

After serving in the U. S. Air Force for four years as an aircraft electronics navigation technician, he attended California State Polytechnic University at Pomona, where he graduated with honors and B.S. degrees in both electrical engineering and physics. He received an M.S. degree in electrical engineering with a minor in acoustics from the Brigham Young University, Provo, Utah, in 1975.

Mr. Keele has worked for a number of audio-related companies in the area of loudspeaker R&D and measurement technology, including Electro-Voice, Klipsch, JBL, and Crown International. He holds three patents on constant-directivity loudspeaker horns. For 11 years he wrote for *Audio* magazine as a senior editor performing loudspeaker reviews. He currently works for Harman-Becker Automotive Systems as a principal engineer in the Advanced Technology Development group.

Mr. Keele has presented and published over 32 technical papers on loudspeaker design and measurement methods and other related topics, among them is the paper, "Low-Frequency Loudspeaker Assessment by Near-Field Sound-Pressure Measurement" (*JAES*, vol. 22, pp. 154-162, 1974 Apr.), for which he won the AES Publications Award. He is a frequent speaker at AES section meetings and workshops and has chaired several AES technical paper sessions. He is an AES fellow (for contributions to the design and testing of low-frequency loudspeakers), a member of the *JAES* Review Board, past member of the AES Board of Governors, and past AES vice president, Central Region USA/Canada. Mr. Keele received the 2001 TEF Richard C. Heyser Award and the Scientific and Technical Academy Award in 2002 from the Academy of Motion Picture Arts and Sciences for his work on cinema constant-directivity loudspeaker systems; and he is listed in the AES Audio Timeline for his pioneer work on the design of constant-directivity high-frequency horns in 1974. He is also a member of the Acoustical Society of America.

Mr. Keele has been married for 34 years, has four children and one grandchild, and resides in Bloomington, Indiana, USA.